Chinese Chemical Letters 34 (2023) 107440

Contents lists available at ScienceDirect

Chinese Chemical Letters

journal homepage: www.elsevier.com/locate/cclet

Metal-free synthesis of pyridyl conjugated microporous polymers with tunable bandgaps for efficient visible-light-driven hydrogen evolution

Zhonghua Cheng, Yan He, Chen Yang, Nan Meng*, Yaozu Liao*

State Key Laboratory for Modification of Chemical Fibers and Polymer Materials, College of Materials Science and Engineering, Donghua University, Shanghai 201620, China

ARTICLE INFO

Article history:
Received 8 February 2022
Revised 2 March 2022
Accepted 14 April 2022
Available online 20 April 2022

Keywords:
Pyridyl conjugated microporous polymers
Metal-free synthesis
Tunable bandgaps
Photocatalysts
Hydrogen evolution reaction

ABSTRACT

Conjugated microporous polymers (CMPs) with tunable bandgaps have attracted increasing attention for photocatalytic hydrogen evolution. However, the synthesis of CMPs usually needs expensive metal-based catalysts. Herein, we report a metal-free synthetic route to fabricate pyridyl conjugated microporous polymers (PCMPs) *via* a condensed polymerization between aldehyde and aryl ketone monomers. The PCMPs show widely tunable specific surface areas (347–418 m^2/g), which were controlled *via* changing the used monomers. The PCMPs synthesized using monomers of dialdehyde and diacetylbenzene (diacetylpyridine) in the presence of pyridine exhibited the highest visible-light driven hydrogen evolution rate (9.56 μmol/h). These novel designed PCMPs provide wide adaptability to current materials designed for high-performance photocatalysts in different applications.

Hydrogen energy is regarded as the most potential clean energy in the 21st century owing to its high combustion heat value and carbon-free emissions. Photocatalytic hydrogen evolution *via* water splitting represents one of the most promising routes for obtaining hydrogen energy [1,2]. To achieve this target, it is required to develop low-cost, efficient, environmentally friendly and stable hydrogen evolution photocatalysts [3,4]. Anatase titanium dioxide (TiO_2), one of the first-generation photocatalyst, has been well studied since 1972 for hydrogen production [5–9]. Many inorganic metal oxides and sulfides such as VO_2, Ga_2O_3, and MoS_2 were then developed for photocatalytic hydrogen production [10–12]. However, these photocatalysts can only be excited under ultraviolet or near-ultraviolet light that occupies only ~4% of the solar light [13,14]. Photocatalysts driven by visible-light (the main part of the solar spectrum) are more promising candidate materials for hydrogen energy.

Recently, polymeric materials have also received wide attention since they possess the merits of finely controllable chemical structures and electronic properties *via* synthetic protocols, which endow them with multiple redox potentials to enable various photocatalytic applications [15–18]. Conjugated polymers, of which the properties can be easily tuned *via* copolymerizing different monomers into conjugated backbones, have also been developed as efficient photocatalysts for visible-light-driven hydrogen evolution [19–21]. However, traditionally used conjugated polymers show linear structures with nonporous characteristics and low surface area. Effective photocatalysts are required to exhibit large surface areas, which can enhance the adsorption of reactants and offer substantial reactive sites. Moreover, large surface areas enable more light to be harvested and also possess continuous pore channels which facilitate the transfer of reactant molecules [22,23].

Conjugated microporous polymers (CMPs), featured with extended π-conjugation, high specific surface area, excellent physicochemical and photocatalytic stability, and tunable chemical structure and electronic properties, have received wide attention as polymeric photocatalysts for hydrogen evolution [24–28]. By controlling chemical structures, bandgaps, and morphologies, series of CMPs have been demonstrated for visible-light-driven hydrogen evolution [29–34]. However, most of the reported CMP materials possess a hydrophobic skeleton, which leads to a poor dispersion in water [35]. The correspondingly CMPs show defective interface between organic photocatalysts and water, which limits the performance of hydrogen evolution. In additions, the current synthetic routes of CMPs usually require precious metal catalysts and harsh reaction conditions [36].

In this work, we present a simple metal-free approach to synthesize a series of pyridyl conjugated microporous polymers (PCMPs) *via* the Chichibabin pyridine reaction between aromatic aldehydes and ketones (Scheme 1). This new synthetic method can be performed at a mild temperature without using expensive metal catalysts, which offers a green route toward hydrogen evolution

* Corresponding authors.
E-mail addresses: n.meng@dhu.edu.cn (N. Meng), yzliao@dhu.edu.cn (Y. Liao).

https://doi.org/10.1016/j.cclet.2022.04.038
1001-8417/

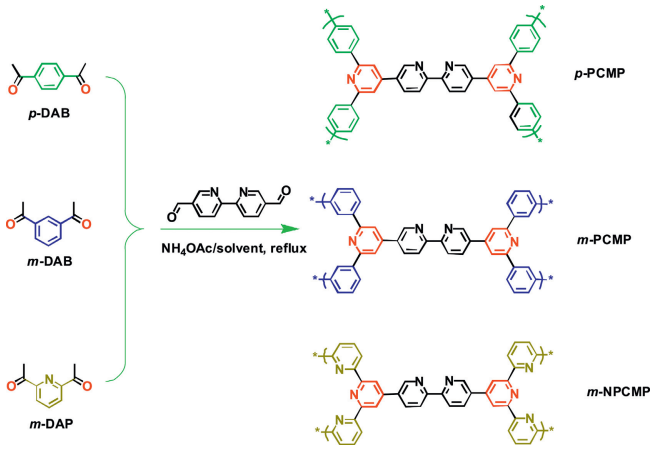

Scheme 1. Synthetic route to PCMPs network.

reaction (HER) photocatalysts. The incorporation of pyridyl nitrogen atoms can improve the wettability of CMPs at the molecular level. The introduction of nitrogen atoms can effectively improve the photo-generated carrier mobility in the system by promoting the rapid propagation of carriers in the π-conjugated structure. By adjusting the nitrogen content, the position and width of the polymer band gap can be changed to tune the photocatalytic activity [37]. Therefore, numerous nitrogen-containing porous polymers, such as covalent organic frameworks (COFs) [38–40], covalent triazine frameworks (CTFs) [41,42], chelating conjugated polymers [43] and CMPs [44–46] have been designed for photocatalysts.

The chemical structure of the as-synthesized polymers was verified using solid-state ^{13}C nuclear magnetic resonance (NMR), Fourier transform infrared (FT-IR), X-ray diffraction (XRD) and X-ray photoelectron spectroscopy (XPS). The solid-state ^{13}C NMR spectra of PCMPs (Fig. 1a) show three peaks at ~154 ppm, ~147 ppm and ~135 ppm, which are ascribed to the pyridyl groups, and the peaks at ~126 ppm and ~120 ppm arise from the phenyl groups. Fig. 1b shows the FT-IR spectra of PCMPs and corresponding monomers. The peak at ~1600 cm^{-1} can be attributed to the C=N bond of the pyridine rings, which indicates the completion of the cyclization reaction. The XRD patterns (Fig. 1c) of PCMPs show broad peaks of amorphous polymers at $2\theta = 20°$, being attributed to π-π interlayer stacking between benzene groups and pyridine groups.

Fig. 1d shows the XPS survey spectra of PCMPs, which confirms the existence of C, N element being consistent with previous results [47]. The C 1s core-level XPS spectra (Fig. 1e) also confirm that two independent peaks at 284.6 eV and 285.4 eV represent C=C and C=N bonds, respectively. The N 1s core-level XPS spectra (Fig. 1f) show a single peak at ~398.7 eV owing to pyridyl N, which also indicates the successful synthesis of PCMPs. The thermogravimetric analysis (TGA) scans (Fig. S1 in Supporting information) demonstrated that the polymer started to decompose at 400 °C, but still maintained 50%–60% at char yields at 1000 °C, which proves the good thermal stability of 3D skeleton of PCMPs.

The N_2 adsorption/desorption isotherms of PCMPs show a typical I/IV type curve, and the adsorption amount of N_2 increased sharply at the low-pressure range ($P/P_0 < 0.5$), which indicates large amounts of microporous structures existed in as-synthesized polymers (Fig. 2a and Fig. S2 in Supporting information). The Brunauer-Emmett-Teller (BET) surface area is up to 418 m^2/g for *m*-PCMP. The pore size distribution of PCMPs is in the range of micropore. In addition, the results of CO_2 and N_2 adsorption of

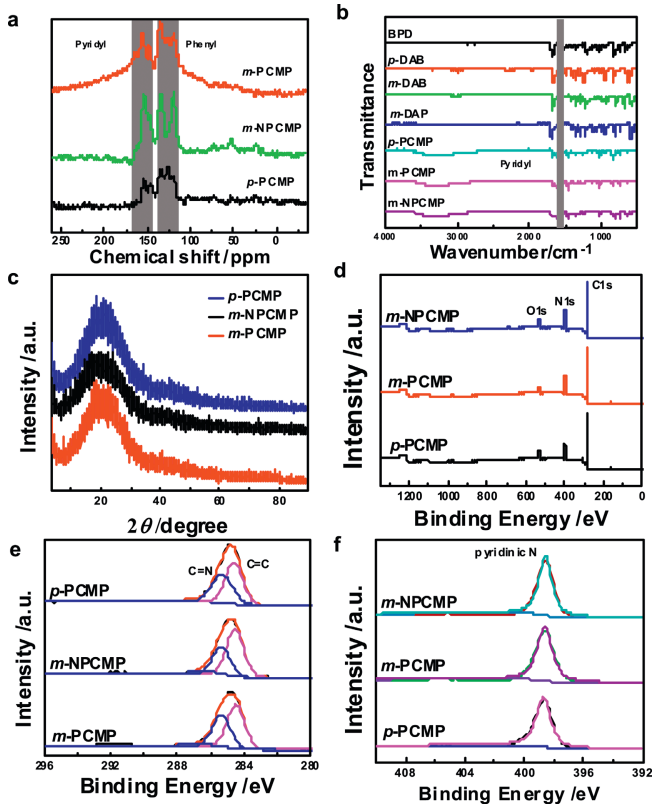

Fig. 1. (a) Solid-state ^{13}C CP/MAS NMR spectra, (b) FT-IR spectra, (c) powder XRD patterns, (d) XPS survey spectra, (e) C 1s core-level XPS spectra, and (f) N 1s core-level XPS spectra of PCMPs.

the PCMPs at 273 K and 298 K further demonstrated the porous structure of PCMPs were consistent with the above results (Figs. 2b and c).

The morphologies of the PCMPs were observed using scanning electron microscopy (SEM) and transmission electron microscopy (TEM) images (Figs. 2d-l). The morphology of the PCMPs obtained from different reaction monomers is similar, demonstrating the uniform sizes of nanoparticles. The particle size of *m*-PCMP is the largest with an avenge diameter of 30 nm, and the accumulation of particles forms mesopores and macropores. HR-TEM further proves that there are a large number of micropores in these three polymers, which is consistent with the results of N_2 adsorption/desorption curve test.

The solid ultraviolet (UV) absorption spectra (Fig. 3a) show the light absorption ranges of PCMPs are similar (200–500 nm). The optical bandgaps estimated from the T_{auc} plot are 2.65 eV-2.71 eV (Fig. 3b) and the conduction band (CB) positions are −1.00 eV to −1.15 eV (Fig. 3c). The calculation results demonstrate that the bandgaps of PCMPs polymers are larger compared to the theoretical bandgaps of water splitting, which indicate that all polymers have sufficient bandgaps for photocatalytic hydrogen evolution reaction, and are expected to be used as photocatalysis of water to produce hydrogen in the visible light range (Table S1 in Supporting informamtion).

The photocatalytic water splitting experiments were performed using PCMPs powders suspended in water with chloroplatinic acid hexahydrate ($H_2PtCl_6{\cdot}6H_2O$) as the co-catalyst and triethanolamine (TEOA) as the hole sacrificial agent. Figs. 3d and e show the photocatalytic hydrogen production in the ultraviolet-visible range of PCMPs. The H_2 production rate of *m*-PCMP, *p*-PCMP and *m*-NPCMP under UV–vis light irradiation ($\lambda > 320$ nm) is 29.86 μmol/h, 25.93 μmol/h and 16.18 μmol/h, respectively, and

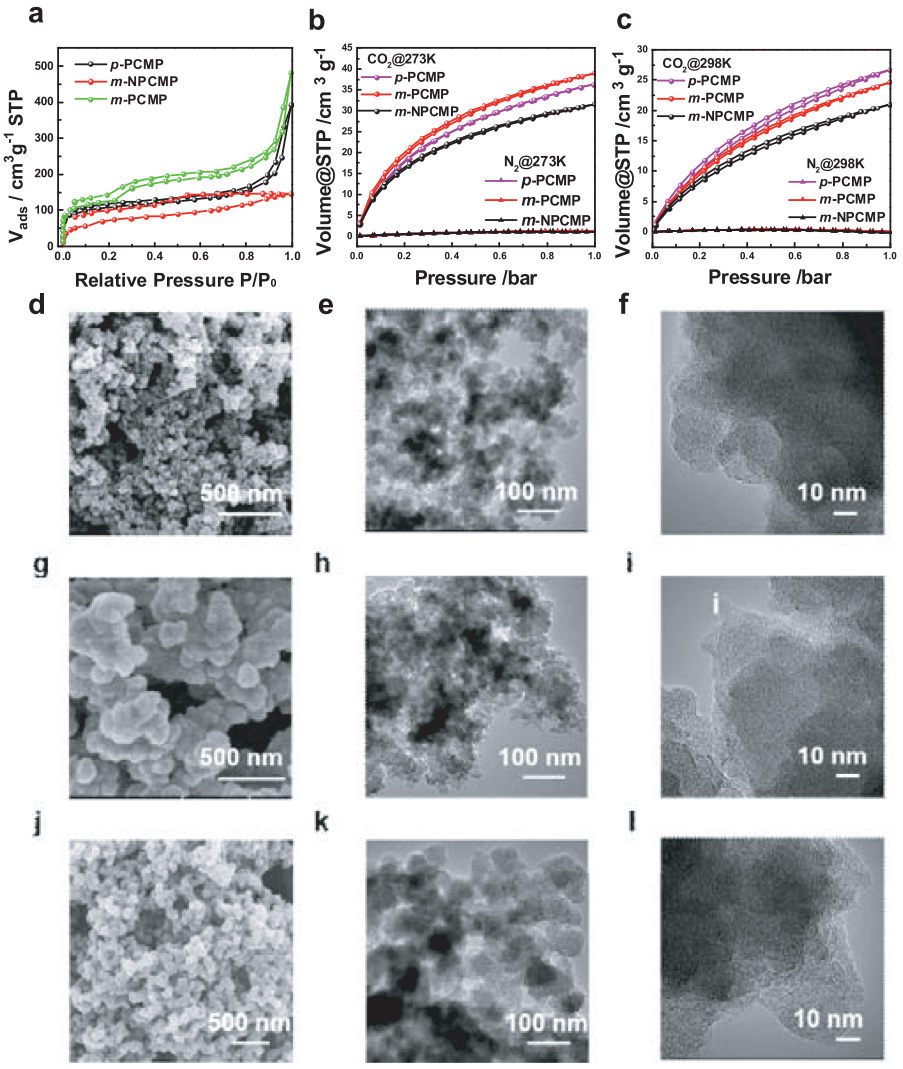

Fig. 2. (a) N_2 adsorption/desorption isotherms, (b, c) CO_2 and N_2 adsorption/desorption isotherms of PCMPs. SEM, TEM and HRTEM images of (d-f) *p*-PCMP, (g-i) *m*-PCMP, and (j-l) *m*-NPCMP.

9.56 μmol/h, 4.72 μmol/h and 1.56 μmol/h under visible light irradiation ($\lambda > 420$ nm), respectively.

These results indicate that the photocatalytic hydrogen producing activity is related to the molecular structure of polymers that the groups in different substitution positions of benzene rings make the differences inactivity. The polymers prepared using different aromatic ketone monomers would have different pore structures. Specifically, *p*-PCMP, formed by the deoxycyclization of para-aromatic aldehyde and para-aromatic ketone, shows relatively regular polymer structure with homogeneous pore size of micropores (~0.6 nm, Fig. S2). Due to the presence of excessive pyridine nitrogen atom, the steric hindrance of 2,6-diacetylpyridine was larger than *para*-aromatic ketone, and the pores formed were smaller after polymerization. The *meta*-aromatic ketone cyclized the polymer to produce pores with different pore sizes. From the pore size distribution curve, it could be seen a large number of micropores and mesopores, which means the polymer had excellent multi-stage pore structure.

Moreover, the different chemical structure results in different electronic structure. In order to evaluate the light stability of the materials, *m*-PCMP was used for continuous photocatalytic hydrogen production for 50 h ($\lambda > 320$ nm), and vacuum degassed every 5 h as a cycle to determine its hydrogen production (Fig. 3f). The polymer exhibits excellent photocatalytic stability, and the photocatalytic hydrogen production rate of the polymer in each cycle was basically maintained at 30.00 μmol/h without significant attenuation. After 40 h of light irradiation, the photocatalytic activity decreased slightly, but still maintained a high hydrogen production capacity, and the photocatalyst could still maintain a high hydrogen production rate of 27.80 μmol/h in the last cycle. After the photocatalytic cycle experiment was completed, we performed an infrared spectrum and scanning electron microscope tests on the recovered samples. As shown in Fig. S3, the structure of the polymer did not change significantly, indicating that *m*-PCMP has excellent light stability and structural stability. In summary, the materials we prepared have excellent hydrogen production activity as photocatalysts, and the hydrogen production rate is higher than that of most organic porous material catalysts (Table S1).

In conclusion, we have synthesized a series of photocatalysts that decompose water to produce hydrogen and discussed the influence of different reaction solvents on catalyst performance. The synthesized PCMPs have excellent porosity and photoelectric properties. The obtained PCMPs demonstrate good photocatalytic hydrogen production activity. Especially, due to the narrower bandgap and richer hierarchical pore structure, *m*-PCMPs show excellent photocatalytic activity in the ultraviolet-visible and visible light range, which the hydrogen production rate is as high as 29.86 and 9.56 μmol/h, respectively. The synthesis method we reported

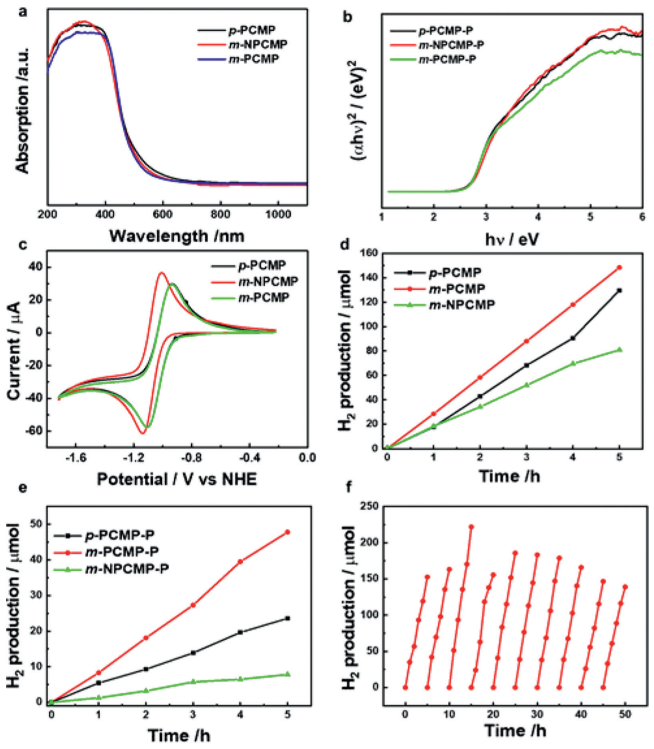

Fig. 3. (a) UV–vis spectra, (b) corresponding T_{auc} plots, (c) photoluminescence emission spectra (λ_{ex} = 380 nm). H_2 production of PCMPs (d) under UV–vis light irradiation (λ > 320 nm), (e) under visible light irradiation (λ > 420 nm), and (f) time course of *m*-PCMP-P under UV–vis light irradiation (λ > 320 nm). Photocatalytic test conditions: 10 mg photocatalyst, 50 mL H_2O, 5 ml TEOA, 3 wt% Pt.

provides a new route to obtain high-efficiency organic semiconductor catalysts suitable for the field of photocatalysis.

Declaration of competing interest

The authors declare that they have no known competing financial interests or personal relationships that could have appeared to influence the work reported in this paper.

Acknowledgments

This work was supported by the National Natural Science Foundation of China (Nos. 52103024, 52073046, 51873036 and 51673039), the Program of Shanghai Academic Research Leader (No. 21XD1420200), the Shanghai Shuguang Program (No. 19SG28), the Chang Jiang Scholar Program (No. Q2019152), the Shanghai Pujiang Talent Program (No. 20PJ1400600), the Shanghai Natural Science Foundation (Nos. 22ZR1401600 and 19ZR1470900), the Fundamental Research Funds for the Central Universities (No. 2232021D-01), and the Fundamental Research Funds for the Central Universities and Graduate Student Innovation Fund of Donghua University (No. CUSF-DH-D-2019024).

Supplementary materials

Supplementary material associated with this article can be found, in the online version, at doi:10.1016/j.cclet.2022.04.038.

References

[1] J. Barber, Chem. Soc. Rev. 38 (2009) 185–196.
[2] A.J. Carrillo, J. Gonzalez-Aguilar, M. Romero, J.M. Coronado, Chem. Rev. 119 (2019) 4777–4816.
[3] X. Zhang, H. Dong, X.J. Sun, et al., ACS Sustain. Chem. Eng. 6 (2018) 11563–11569.
[4] C. Sundaram, Y. Lei, D. Libo, et al., Chem. Soc. Rev. 8 (2019) 4178–4280.
[5] A. Fujishima, K. Honda, Nature 238 (1972) 37–38.
[6] X. Chen, S. Shen, L. Guo, S.S. Mao, Chem. Rev. 110 (2010) 6503–6570.
[7] L. Liu, X. Gu, Z. Ji, et al., J. Phys. Chem. C 117 (2013) 18578–18587.
[8] L. Liu, Z. Ji, W. Zou, et al., ACS Catal. 3 (2013) 2052–2061.
[9] A. Kudo, Y. Miseki, Chem. Soc. Rev. 38 (2009) 253–278.
[10] X.B. Chen, S.H. Shen, L.J. Guo, S.S. Mao, Chem. Rev. 110 (2010) 6503–6570.
[11] R.S. Sprick, J.X. Jiang, B. Bonillo, et al., J. Am. Chem. Soc. 137 (2015) 3265–3270.
[12] G. Ye, Y. Gong, J. Lin, et al., Nano Lett. 16 (2016) 1097–1103.
[13] A. Fujishima, X.T. Zhang, D.A. Tryk, Surf. Sci. Rep. 63 (2008) 515–582.
[14] A. Meng, L. Zhang, B. Cheng, J. Yu, Adv. Mater. 31 (2019) 1807660.
[15] M.G. Schwab, M. Hamburger, X. Feng, et al., Chem. Commun. 46 (2010) 8932–8934; S. Sprick, B. Bonillo, R. Clowes, et al., Angew. Chem. Int. Ed. 57 (2018) 2520.
[16] M. Sachs, R.S. Sprick, D. Pearce, et al., Nat. Commun. 9 (2018) 4968.
[17] M. Aitchison, R.S. Sprick, A.I. Cooper, J. Mater. Chem. A 7 (2019) 2490–2496.
[18] Z.A. Lan, G. Zhang, X. Chen, et al., Angew. Chem. Int. Ed. 58 (2019) 10236–10240.
[19] S. Sprick, C.M. Aitchison, E. Berardo, et al., J. Mater. Chem. A 6 (2018) 11994–12003.
[20] Y. Wang, Y. Di, M. Antonietti, et al., Chem. Mater. 22 (2010) 5119–5121.
[21] H. Yu, R. Shi, Y. Zhao, et al., Adv. Mater. 29 (2017) 1605148.
[22] J. Chen, C.L. Dong, D. Zhao, et al., Adv. Mater. 29 (2017) 1606198.
[23] G. Zhou, L.L. Zheng, D. Wang, et al., Chem. Commun. 55 (2019) 4150–4153.
[24] M. Luo, Q. Yang, K. Liu, H. Cao, H. Yan, Chem. Commun. 55 (2019) 5829–5832.
[25] A.Acharjya Kuecken, L. Zhi, et al., Chem. Commun. 53 (2017) 5854–5857.
[26] Z.A. Lan, Y. Fang, X. Chen, X. Wang, Chem. Commun. 55 (2019) 7756–7759.
[27] W. Huang, Q. He, Y. Hu, Y. Li, Angew. Chem. Int. Ed. 131 (2019) 1–6.
[28] K. Wang, L.M. Yang, X. Wang, et al., Angew. Chem. Int. Ed. 56 (2017) 14149–14153.
[29] L. Guo, Y. Niu, H. Xu, et al., J. Mater. Chem. A 6 (2018) 19775–19781.
[30] C.B. Meier, R.S. Sprick, A. Monti, et al., Polymer (Guildf) 126 (2017) 283–290.
[31] Y.S. Kochergin, D. Schwarz, A. Acharjya, et al., Angew. Chem. Int. Ed. 57 (2018) 14188–14192.
[32] K.Schwinghammer Stegbauer, B.V. Lotsch, Chem. Sci. 5 (2014) 2789–2793.
[33] S. Vyas, F. Haase, L. Stegbauer, et al., Nat. Commun. 6 (2015) 8508.
[34] X. Wang, L. Chen, S.Y. Chong, et al., Nat. Chem. 10 (2018) 1180.
[35] P. Pachfule, A. Acharjya, J.R.M. Roeser, et al., J. Am. Chem. Soc. 140 (2018) 1423–1427.
[36] J.L. Sheng, H. Dong, X.B. Meng, et al., ChemCatChem 11 (2019) 2313–2319.
[37] C. Bie, H. Yu, B. Cheng, et al., Adv. Mater. 33 (2021) 2003521.
[38] S.B.P. Thiruvengadam, S. Wei, W. Zhang, et al., J. Am. Chem. Soc. 142 (2020) 11893–11900.
[39] S. Bi, C. Yang, W. Zhang, et al., Nat. Commun. 10 (2019) 2467.
[40] S. Bi, Z. Lan, S. Paasch, et al., Adv. Funct. Mater. 27 (2017) 1703146.
[41] S. Zhang, G. Cheng, L. Guo, et al., Angew. Chem. Int. Ed. 59 (2020) 6007–6014.
[42] L. Guo, X. Wang, Z. Zhan, et al., Chem. Mater. 33 (2021) 1994–2003.
[43] L. Li, R.G. Hadt, S. Yao, et al., Chem. Mater. 28 (2016) 5394–5399.
[44] C. Yang, Z. Cheng, G. Divitini, et al., J. Mater. Chem. A 9 (2021) 18674–19900.
[45] Y. He, Z. Cheng, H. Zuo, C. Yan, Y. Liao, ChemElectroChem 7 (2020) 959–966.
[46] Q. Zeng, Z. Cheng, C. Yang, et al., Chin. J. Polym. Sci. 39 (2021) 1004–1012.
[47] Z. Cheng, L. Wang, Y. He, et al., Polym. Chem. 11 (2020) 3393–3397.